JOURNAL OF VIROLOGY, June 1993, p. 3048–3060
0022-538X/93/063048-13$02.00/0
Copyright © 1993, American Society for Microbiology
Vol. 67, No. 6

# Role of Conserved Glycosylation Sites in Maturation and Transport of Influenza A Virus Hemagglutinin

PAUL C. ROBERTS, WOLFGANG GARTEN,* AND HANS-DIETER KLENK

*Institut für Virologie, Philipps-Universität Marburg, Robert-Koch-Strasse 17, D-3550 Marburg, Germany*

Received 7 December 1992/Accepted 22 February 1993

**The role of three N-linked glycans which are conserved among various hemagglutinin (HA) subtypes of influenza A viruses was investigated by eliminating the conserved glycosylation (cg) sites at asparagine residues 12 (cg1), 28 (cg2), and 478 (cg3) by site-directed mutagenesis. An additional mutant was constructed by eliminating the cg3 site and introducing a novel site 4 amino acids away, at position 482. Expression of the altered HA proteins in eukaryotic cells by a panel of recombinant vaccinia viruses revealed that rates and efficiency of intracellular transport of HA are dependent upon both the number of conserved N-linked oligosaccharides and their respective positions on the polypeptide backbone. Glycosylation at two of the three sites was sufficient for maintenance of transport of the HA protein. Conserved glycosylation at either the cg1 or cg2 site alone also promoted efficient transport of HA. However, the rates of transport of these mutants were significantly reduced compared with the wild-type protein or single-site mutants of HA. The transport of HA proteins lacking all three conserved sites or both amino-terminally located sites was temperature sensitive, implying that a polypeptide folding step had been affected. Analysis of trimer assembly by these mutants indicated that the presence of a single oligosaccharide in the stem domain of the HA molecule plays an important role in preventing aggregation of molecules in the endoplasmic reticulum, possibly by maintaining the hydrophilic properties of this domain. The conformational change observed after loss of all three conserved oligosaccharides also resulted in exposure of a normally mannose-rich oligosaccharide at the tip of the large stem helix that allowed its conversion to a complex type of structure. Evidence was also obtained suggesting that carbohydrate-carbohydrate interactions between neighboring oligosaccharides at positions 12 and 28 influence the accessibility of the cg2 oligosaccharide for processing enzymes. We also showed that terminal glycosylation of the cg3 oligosaccharide is site specific, since shifting of this site 4 amino acids away, to position 482, yielded an oligosaccharide that was arrested in the mannose-rich form. In conclusion, carbohydrates at conserved positions not only act synergistically by promoting and stabilizing a conformation compatible with transport, they also enhance trimerization and/or folding rates of the HA protein.**

A common modification of many secretory and most integral membrane proteins in the exocytic pathway is attachment of preformed oligosaccharides to asparagine residues residing in the consensus sequence Asn-X-Thr/Ser, where X can be any amino acid except proline (28). Numerous functions for N-linked glycans have been implicated, including (i) promotion of proper folding, (ii) maintenance of protein conformation and stability, (iii) protection against denaturation and proteolysis, and (iv) modulation of biological activities (46, 47, 56). Results from experiments using the antibiotic tunicamycin, which blocks N-glycosylation by interfering with the assembly of lipid-linked precursor oligosaccharides, have suggested that the requirement for N-glycosylation is intrinsic to a given protein. Some proteins are transported and function normally when glycosylation is inhibited with tunicamycin, whereas others exhibit folding defects, frequently resulting in protein aggregation in the endoplasmic reticulum (ER) or rapid degradation of nonglycosylated proteins (13, 55).

The vast amount of structural information available about various influenza virus hemagglutinin (HA) subtypes, including the three-dimensional structure of the HA and various deduced amino acid sequences, has led to the use of HA as a model integral type 1 glycoprotein to examine factors governing the maturation and transport of proteins in the exocytotic pathway. Like cellular glycoproteins, HA is synthesized on membrane-bound ribosomes and translocated into the lumen of the ER, where signal peptide cleavage and core glycosylation occur. During its intracellular transport, HA undergoes extensive posttranslational modifications, including trimerization (3, 4, 8, 9, 16), fatty acid acylation (41, 59, 63), trimming and processing of the N-linked glycans (23), and proteolytic cleavage into the disulfide-bound $HA_1$ and $HA_2$ subunits (extensively reviewed in reference 27).

Amino acid sequence analysis has revealed that there is considerable variation in both the number and location of potential glycosylation sites among different HA subtypes (H1 to H14) and even among variants from a single subtype (22, 43). However, two potential glycosylation sites, at Asn-12 and Asn-478 (H7 numbering), are highly conserved and a further site, at Asn-28, is semiconserved, meaning that this glycosylation site is absent in serotypes H4, H8, H9, and H12 (43). Whereas the oligosaccharides found at variable sites, that are scattered throughout the molecule with a prevalence in the upper globular domain, have been shown to modulate antigenic properties (25, 40, 57), receptor binding (51), and proteolytic activation (20, 21, 44, 45), the functional importance of carbohydrates at the conserved sites has yet to be defined. The conserved glycosylation sites are located within the stem region of the HA molecule, which has been assumed to provide the main forces that stabilize the HA trimer (16, 65, 66). Although loss of single conserved carbohydrate attachment sites has been described

* Corresponding author.

before (39, 48), combined removal of several of these sites has not been studied.

In this study, we eliminated the conserved carbohydrates at one or more glycosylation sites by site-specific mutagenesis and examined the maturation and transport of the resulting HA mutants. We established that the number of conserved oligosaccharides and their positions in the molecule influence trimerization and rates and efficiency of transport and contribute to the stability of the HA protein. Loss of all three conserved sites resulted in temperature sensitivity of transport, whereas loss of carbohydrates at two of the three sites significantly reduced rates of transport. We conclude that the conserved oligosaccharides function in a cooperative manner in enhancing and stabilizing a transport-competent form of HA. In addition, we were able to show that oligosaccharides at conserved sites in the stem domain of the molecule influence the final structures of specific oligosaccharides, either by carbohydrate-carbohydrate interference or by stabilizing a conformation of the HA, which affects the accessibility of an oligosaccharide for processing enzymes.

(This work was done by P. C. Roberts in partial fulfillment of the requirements for a Ph.D. degree from the Philipps-Universität, Marburg, Germany. The data reported here were presented at the Negative Strand Viruses 8th International Conference, Charleston, S.C., 15 to 20 September 1991.)

## MATERIALS AND METHODS

**Cells and viruses.** CV-1 cells were grown in Dulbecco's medium supplemented with 5% fetal calf serum. For expression studies, the CV-1 cells were cultured in 35-mm-diameter culture dishes (GIBCO, Eggenstein, Germany) or on glass coverslips in 24-well culture plates. The WR strain of vaccinia virus was propagated in CV-1 cells and isolated as described previously (36). Human $TK^-$143 cells were grown in Dulbecco's medium supplemented with 5% fetal calf serum and 25 μg of 5-bromodeoxyuridine (Sigma, Taufkirchen, Germany) per ml.

**Oligonucleotide-directed mutagenesis and construction of recombinant vaccinia viruses.** The construction of recombinant M13mp11-HA, containing the cDNA of the HA gene from influenza virus strain A/FPV/Rostock/34 (H7N1) (29), has been described previously (63). Four synthetic oligonucleotide primers were designed so that at each consensus sequence for N-linked glycosylation, Asn-X-Thr/Ser, the Thr-encoding codons would be substituted for Ala-encoding codons, and in one case this substitution was accompanied by the exchange of an Asp-encoding codon for Asn, resulting in a novel site 4 amino acids away from the original glycosylation site. Mutagenesis was carried out by the method originally described by Taylor and coworkers (62), by using a commercially available in vitro mutagenesis kit (Amersham-Buchler, Braunschweig, Germany). Single-site glycosylation mutants were subjected to further rounds of mutagenesis to generate double- and triple-site mutants. Mutants were verified by the dideoxynucleotide chain termination sequencing method (53). The coding sequences of wild-type HA and HA mutants were excised from the bacteriophage replicative-form DNA with *Bgl*II and ligated to pSC11 (5). Transfection and isolation of recombinant viruses were performed essentially as previously described (36).

**Infection of CV-1 cells with recombinant vaccinia virus and metabolic labeling of infected cells.** For all labeling experiments, CV-1 cells were infected with recombinant vaccinia virus at 10 PFU per cell at 37°C. Prior to labeling, the cells were incubated in methionine-free Dulbecco's modified Eagle's medium for 2.5 h at 37, 33, or 40°C. Unless otherwise indicated, cells were pulse-labeled at 3.5 h postinfection with 100 μCi of L-[$^{35}$S]methionine (Amersham-Buchler) per ml (1,000 Ci/mmol) for 10 min at the appropriate temperature and the radioactive label was chased for various times up to 2 h by adding unlabeled L-methionine to a final concentration of 20 mM. Following the chase, the cells were lysed on ice with 400 μl of either RIPA buffer (1% Triton X-100, 1% deoxycholate, 0.1% sodium dodecyl sulfate [SDS], 0.15 M NaCl, 20 mM Tris, 10 mM EDTA, 10 mM N-ethylmaleimide [Sigma], 1 mM phenylmethylsulfonyl fluoride [Sigma]) or Triton lysis buffer containing 1% Triton X-100 in MNT [20 mM 2-(*N*-morpholino)ethanesulfonic acid (MES; Sigma), 100 mM NaCl, 30 mM Tris-HCl (pH 7.5), 20 mM N-ethylmaleimide] supplemented with 1 mM EDTA (Sigma) and 1 mM phenylmethylsulfonyl fluoride. Chymostatin, pepstatin, leupeptin, and antipain (Sigma) were routinely included as protease inhibitors (10 μg/ml) in each lysis buffer. Nuclei were removed by centrifugation for 20 min at 13,000 × *g*. The supernatants (cell extracts) were used immediately for cross-linking experiments, velocity gradient centrifugation, or immunoprecipitation.

**Chemical cross-linking with DSP and velocity gradient centrifugation.** To 100-μl aliquots of cell extracts lysed in Triton lysis buffer, 2 μl of a freshly prepared solution of dithiobis(succinimidylpropionate) (Pierce Chemical Co., BA, Oud Beijerland, The Netherlands) (40 mM) in dimethyl sulfoxide was added, and the samples were incubated at 15°C for 15 min. The reaction was stopped by addition of 2 μl of 1 M ammonium hydrogen carbonate, and the samples were subjected to immunoprecipitation (15). Control samples were incubated under the same conditions with only dimethyl sulfoxide as a negative control. Velocity gradient centrifugation was performed essentially as described before (16, 30).

**Endo H and PGNase F digestions.** Endoglycosidase H (endo H) and *N*-glycosidase F (PNGase F) digestions were performed on immunoprecipitated proteins derived from 200-μl aliquots of the cell extract. After the final wash, precipitates were suspended in 30 μl of 50 mM phosphate buffer, pH 7.0, containing 0.5% mercaptoethanol and 0.1% SDS and heated to 95°C for 3 min. Protein A-Sepharose CL4B was pelleted by centrifugation for 5 min at 13,000 × *g*, and the supernatants were divided into three 10-μl aliquots. The aliquots received either 1 mU of endo H or PNGase F (Boehringer, Mannheim, Germany) or served as a control. Digestions were performed for 16 h at 37°C (40), after which 10 μl of 2× gel sample buffer was added and samples were incubated at 95°C for 5 min. The digested material was subjected to SDS-polyacrylamide gel electrophoresis (PAGE) and fluorography.

**Indirect immunofluorescence.** Confluent CV-1 cells, cultured on glass coverslips, were infected with recombinant vaccinia virus for 6 h at 33, 37, or 40°C. After incubation at the respective temperatures, cells were fixed with 2% paraformaldehyde in phosphate-buffered saline (PBS) for 10 min. Fixation was quenched with 0.1 M glycine in PBS for 15 min. For intracellular staining, the cells were treated with 0.3% Triton X-100 for 15 min and then extensively washed with PBS. Both the first (anti-fowl plague virus [FPV]) and the second (rhodamine-conjugated swine anti-rabbit immunoglobulins or fluorescein-conjugated goat anti-rabbit immunoglobulins [Dakopats, Hamburg, Germany]) antibodies were diluted 1:100 in PBS containing 3% bovine serum

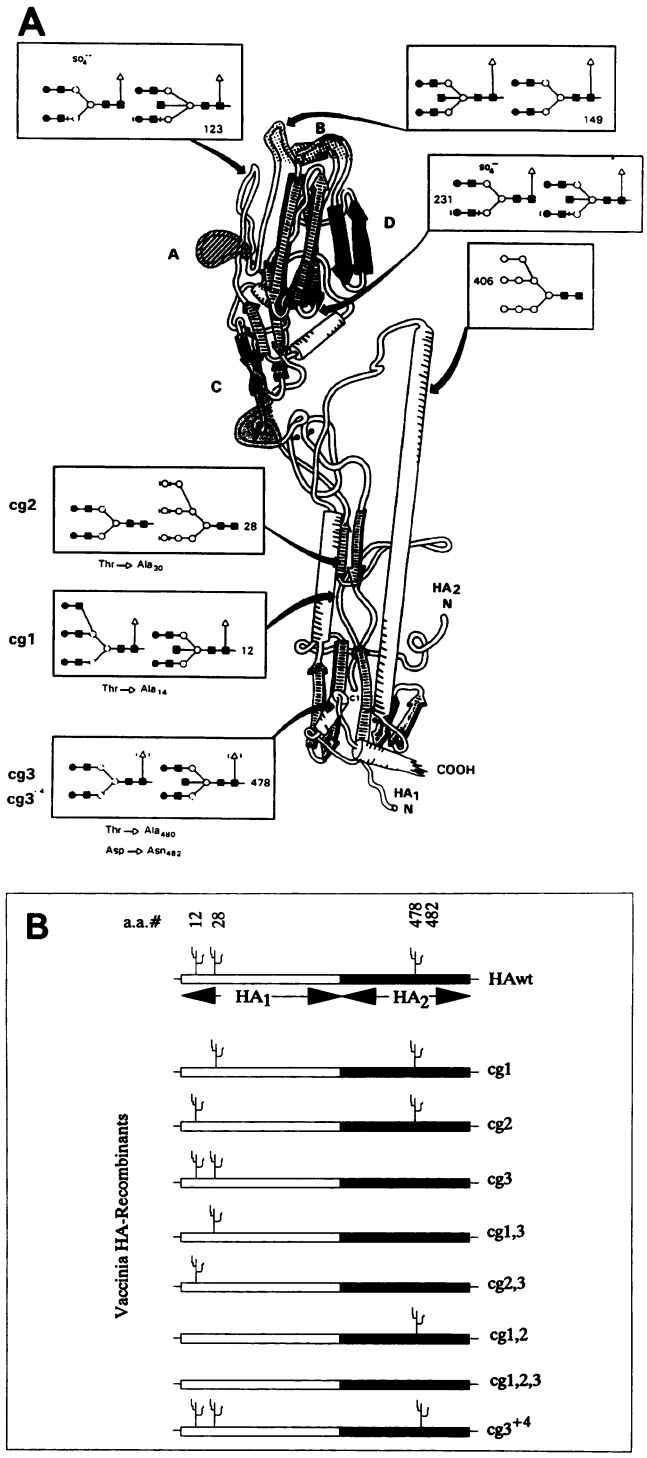


FIG. 1. Depiction of the HA monomer and schematic representation of HA glycosylation mutants generated by site-directed mutagenesis. (A) Drawing of the HA monomer (66) showing the carbohydrate structures present at the seven glycosylation sites of the HA of influenza virus strain A/FPV/Rostock/34 (H7N1) (23). The positions of the asparagine residues are indicated in accordance with the H7 HA amino acid sequence (50). The conserved glycosylation sites are designated cg1 (Asn-12) and cg2 (Asn-22) in the $HA_1$ subunit and cg3 (Asn-478) in the $HA_2$ subunit and correspond to H3 numbering as residues 22, 38, and 483, respectively. (B) Vaccinia virus HA recombinants are characterized by loss of one or more of the conserved glycosylation sites. The designated name is at the right of each diagram. The HA wild type (HAwt) is shown at the top, the $HA_1$ subunit is indicated by the hollow bar, the $HA_2$ subunit is indicated by the black bar, and conserved sites for N-linked glycosylation are indicated by tree-like symbols at Asn residues numbered as in panel A. a.a., amino acid.

albumin prior to incubation with infected cells. Unbound antibodies were removed after each successive incubation period by extensive washing with PBS, and coverslips were mounted in Fluoroprep (bioMerieux, Marcy l'Etoile, France). Fluorescence was examined with the Zeiss Axiophot microscope equipped with UV optics.

## RESULTS

**Elimination of conserved sites for N-linked glycosylation.** Oligonucleotide-directed mutagenesis was employed to examine the functional importance of the conserved sites for N-glycosylation in the intracellular maturation and transport of HA. Shown in Fig. 1A is a drawing of the ectodomain of the HA monomer (66) depicting the locations and the structures of individual carbohydrates found at each of the seven glycosylation sites for the HA of influenza virus strain A/FPV/Rostock/34 (H7N1) (23). Conserved glycosylation sites are designated cg1 at Asn-12, cg2 at Asn-28, and cg3 at Asn-478. Seven glycosylation mutants were constructed by site-directed mutagenesis and inserted into vaccinia virus insertion vector pSC11. Since it has been previously suggested that loss of the oligosaccharide at the cg3 site (39) or introduction of a supernumerary glycosylation site in this region of the molecule (14, 54) can lead to temperature-sensitive transport of HA, we constructed an additional mutant, the $cg3^{+4}$ mutant, by eliminating the cg3 glycosylation site and introducing a novel site at Asn-482, 4 amino acids away from the original site (Fig. 1A and B). The recombinant plasmids were then used to transfect CV-1 cells infected with vaccinia virus, and high-titer virus stocks were prepared from the resulting recombinant viruses, which contain the mutant HA coding sequences inserted into the vaccinia virus genome. The recombinants are designated on the basis of loss of one or more conserved glycosylation sites (Fig. 1B).

**Expression of HA glycosylation mutants.** To confirm expression of the wild-type HA and mutant proteins initially, CV-1 cells infected with recombinant vaccinia virus were labeled with [$^{35}$S]methionine. HA polypeptides were immunoprecipitated with an anti-FPV serum and analyzed by SDS-PAGE and fluorography (Fig. 2). Except for the $cg3^{+4}$ mutant, all of the mutant HA proteins showed an increased rate of mobility compared with wild-type HA, corresponding to the absence of one or more oligosaccharide chains at the conserved glycosylation sites. The absence of oligosaccharides on these mutants is more apparent after intracellular cleavage of the precursor HA resulting in the $HA_1$ and $HA_2$ subunits. As expected for the single-site glycosylation mutants, increased mobility was observed in the $HA_1$ subunit of cg1 and cg2 mutants and in the $HA_2$ subunit of the cg3 mutant. The diminished labelling of $HA_1$ of cg3 and $cg3^{+4}$ mutants can be explained by shedding of $HA_1$ into the medium, as shown for the wild type (see Fig. 6). Double- and triple-site mutants displayed similar increased mobility in their subunits, commensurate with the loss of one or two glycosylation sites in their $HA_1$ subunits and/or one site in their $HA_2$ subunits. Since intracellular cleavage is a normal

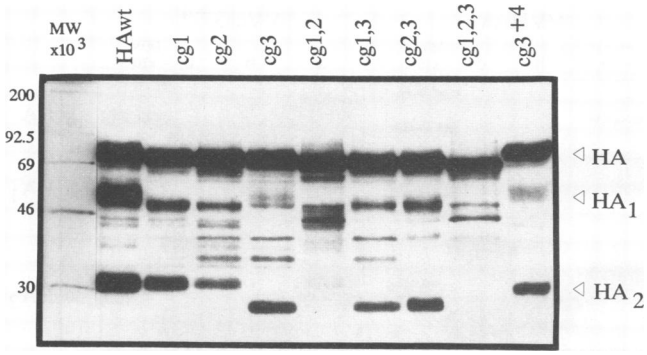


FIG. 2. Expression of HA glycosylation mutants. Recombinant vaccinia virus-infected CV-1 cells (35-mm dishes) were metabolically labeled at 3.5 h postinfection with [$^{35}$S]methionine (20 μCi/ml) for 2 h at 37°C. Detergent extracts (radioimmunoprecipitation assay) of labeled proteins were immunoprecipitated with anti-FPV serum and analyzed by SDS–10% PAGE (31) and fluorography. The positions of uncleaved HA and cleaved subunits HA$_1$ and HA$_2$ are indicated at the right, and those of $^{14}$C-labeled molecular weight (MW) markers are on the left. HAwt, wild-type HA.

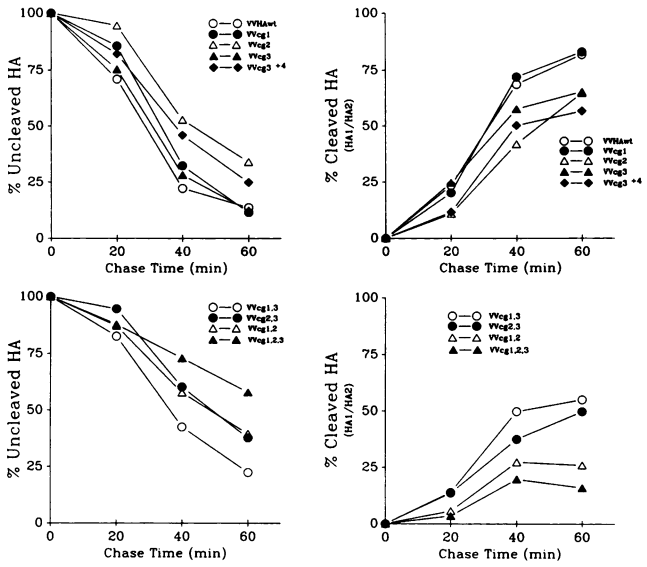


FIG. 3. Kinetics of intracellular transport as determined by rate of cleavage. Recombinant vaccinia virus (VV)-infected CV-1 cells were pulse-labeled with [$^{35}$S]methionine for 10 min at 37°C. The cells were harvested immediately or chased in the presence of excess unlabeled methionine for the times indicated. Aliquots from cell extracts were immunoprecipitated with anti-FPV serum and subjected to SDS–10% PAGE and fluorography. Quantitation of the individual HA bands was done as described in Materials and Methods. The results represent the mean values for the times indicated from at least three independent pulse-chase experiments for each recombinant. Upper panels: quantitation of the single-site mutants and the wild-type HA recombinant. Lower panels: quantitation of double- and triple-site HA glycosylation mutants. The decline in the percentage of uncleaved HA (left panels) and the subsequent increase in the amounts of cleaved HA (right panels) are shown. Cleaved HA was calculated as the amount of radioactivity derived from the HA$_2$ bands at each time period and extrapolated to total cleaved HA. HAwt, wild-type HA.

processing event in the maturation of FPV HA (26), it is apparent that the vaccinia virus cg1,2- and cg1,2,3 mutant-expressed proteins are defective in terms of cleavage. The decreased levels of cleaved HA produced by these mutants, compared with wild-type HA, suggests that either the transport of these proteins is impaired, as shown for various FPV mutants (15, 33, 39, 54), or these proteins have acquired a conformation which does not allow proper access of the enzyme responsible for HA cleavage.

**Kinetics of intracellular transport of wild-type HA and the HA glycosylation mutants.** Cleavage of HA by the endoprotease furin (60) occurs late in transport, probably in the trans region of the Golgi apparatus or in the trans-Golgi network (2, 10, 37, 60). Monitoring cleavage of the FPV HA therefore provides a relatively simple assay for determining whether mutations affect the transit time of newly synthesized FPV HA from the ER to late Golgi compartments. The rate of cleavage of each mutant was determined in pulse-chase experiments and compared with that of wild-type HA. After SDS-PAGE and fluorography of immunoprecipitated HA proteins, the uncleaved precursor form of HA and the HA$_2$ cleavage product, which migrates as a well-resolved band, were quantitated by liquid scintillation counting. The proportion of radioactivity in the HA$_2$ subunit was extrapolated to represent total cleaved HA (HA$_1$/HA$_2$).

Examination of the results from the expression of single-site recombinants (Fig. 3, upper panel) reveals that the rate at which VVcg1- and VVcg3-expressed proteins were cleaved was similar to that of expressed wild-type HA, with a half-time of 30 min. However, the HA proteins expressed by the vaccinia virus cg2 and cg3$^{+4}$ recombinants were cleaved at slower rates (half-times, ~45 and 41 min, respectively), suggesting that loss of the carbohydrate at the Asn-28 site or the presence of a carbohydrate at the abnormal position at Asn-482 interferes with rapid formation of a transport-competent form of the HA early after synthesis. However, these mutations did not seem to affect the yield of the transported HA when the chase time was prolonged to 120 min (data not shown), suggesting that carbohydrate on the remaining conserved sites compensates for these changes. The functional relevance of the carbohydrate at Asn-28 is emphasized by the data obtained with the multiple-site mutants (Fig. 3, lower panel). Here, it is evident that in the absence of carbohydrates at conserved sites cg1 and cg3, the presence of the cg2 oligosaccharide (vaccinia virus cg1,3 mutant) alone can promote a transport-competent form of the HA. A carbohydrate at the cg1 site alone (vaccinia virus cg2,3 mutant) can also compensate for loss of the other two conserved sites. As expected from the experiments described in Fig. 2, the most adverse effects on the kinetics of transport were observed after loss of the two conserved sites in the HA$_1$ subunit (vaccinia virus cg1,2 mutant) and after loss of all three conserved sites for glycosylation (vaccinia virus cg1,2,3 mutant). Cleavage of these HA proteins leveled off after 40 min of the chase, suggesting that only portions of these molecules (35 and 17% of the cg1,2 and cg1,2,3 HA proteins, respectively) are transport competent at 37°C. Since sequential removal of oligosaccharides at the conserved sites for glycosylation differentially retarded transport, it appears that there is a cooperative effect between the conserved oligosaccharides in promoting or stabilizing transport-competent forms of HA protein. Carbohydrate-deficient mutants which had lost the cg2 site showed the most impaired HA transport, even when the cg2 site alone had been eliminated. In addition, HA trimerization, as analyzed by cross-linking kinetics, was about twofold slower with the cg2 oligosaccharide-deficient mutants than with wild-type HA (Fig. 4). Taken together, it seems that the cg2 oligosac-

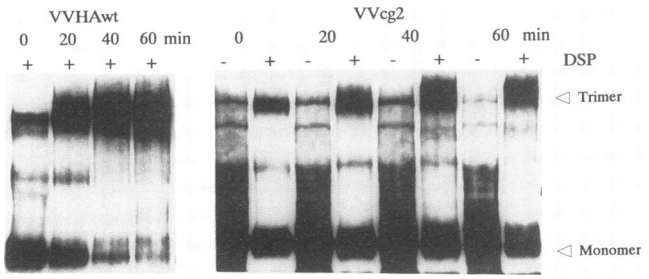


FIG. 4. Oligomerization of HA recombinant proteins. Recombinant vaccinia virus (VV)-infected cells were metabolically pulse-labeled and chased in an experiment similar to that described in the legend to Fig. 2, except that the cells were lysed in Triton lysis buffer. Two aliquots at each time period were incubated either with (+) or without (−) the chemical cross-linking agent dithiobis(succinimidylpropionate) (DSP) for 15 min at 15°C. Reactions were quenched by addition of 1 M ammonium hydrogen carbonate, and the HA-specific proteins were immunoprecipitated with anti-FPV serum and subjected to SDS–6% PAGE under nonreducing conditions, followed by fluorography. Shown are the results obtained with recombinant vaccinia virus-expressed wild-type HA (HAwt) and the cg2 mutant (the dimethyl sulfoxide control was omitted for wild-type HA). The positions of the HA monomer and trimer migrating bands are indicated at the right.

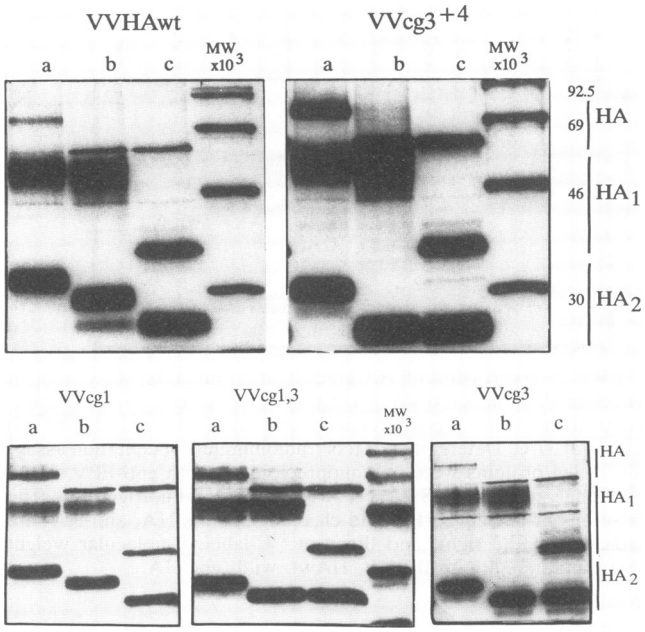


FIG. 5. Oligosaccharide trimming and processing of HA proteins. Aliquots of CV-1 cell extracts, derived from pulse-chase experiments with cells infected with the vaccinia virus (VV) wild-type HA (HAwt), cg1, cg3, cg1,3, and cg3$^{+4}$ recombinants (see the legend to Fig. 3) were immunoprecipitated with anti-FPV serum and left untreated (lanes a) or were digested with endo H (lanes b) to cleave oligomannosidic side chains or with PNGase F (lanes c) to remove both complex- and oligomannosidic-type oligosaccharide side chains. Molecular weight (MW) markers are as in Fig. 2.

charide plays a dominant role in promoting trimerization and transport of FPV HA. The slower rates of trimerization and cleavage of the mutant HA proteins are probably indicative of altered folding rates by these mutants. Thus, the rate and efficiency of formation of transport-competent molecules appear to be dependent on carbohydrate at one or more of the conserved glycosylation sites.

**Processing of the oligosaccharide chains of HA.** To establish that cleavage of mutant HA proteins is not the result of unspecific proteolysis that occurs before terminal glycosylation, the HA polypeptides were treated with endo H and PNGase F after pulse-chase labeling with [$^{35}$S]methionine. Resistance to endo H also provides a suitable way to measure the transit of glycoproteins from the ER to medial Golgi cisternae (28). Furthermore, by comparing the endo H profiles of the vaccinia virus-expressed HA proteins with the predicted carbohydrate structures for FPV-expressed HA (Fig. 1A), it should be possible to validate the proposed conformational restrictions placed on the processing of individual oligosaccharides of the HA (23).

The increased mobilities of the subunits of the wild-type HA protein after endo H and PNGase F treatment seen in Fig. 5 correspond well to the results derived from the structural analysis of the individual oligosaccharides found at each of the seven glycosylation sites for the FPV HA (23). Thus, whereas the $HA_1$ subunit is largely composed of complex endo H-resistant structures at sites 12, 28, 123, 149, and 231, the $HA_2$ subunit possesses a complex endo H-resistant oligosaccharide at Asn-478 and an oligomannosidic structure at Asn-406 (Fig. 1A). The oligosaccharide at Asn-406, which is located in niches of the HA trimer, is inaccessible for processing enzymes, owing to the conformation of the trimer (24). The small shift in the electrophoretic mobility of the $HA_1$ subunit of wild-type HA after endo H treatment is also consistent with these results and can be attributed to the finding that a significant portion of the structures found at the Asn-28 site are of the oligomannosidic type. The presence of both oligomannosidic- and complex-type structures at this site was suggested to be due to partial steric hindrance, by virtue of the adjacent oligosaccharide at the Asn-12 site (23). Analysis of the $HA_1$ subunits of vaccinia virus cg1 and cg3 mutant expressed proteins after endo H treatment (Fig. 5) showed that this proposed effect of steric hindrance can be alleviated after loss of the oligosaccharide at Asn-12 but not after loss of the cg3 oligosaccharide. Thus, the cg1-cg2 carbohydrate interactions interfere with the accessibility of the carbohydrate at Asn-28 to processing enzymes.

Figure 5 shows also that unlike wild-type HA and the cg1 mutant, the cg3$^{+4}$ mutant has an $HA_2$ carbohydrate complement completely sensitive to endo H treatment. Thus, the cg3$^{+4}$ mutant has an oligomannosidic oligosaccharide not only at Asn-406 but also at Asn-482. The fact that the normal cg3 site at Asn-478, which is only 4 amino acids away, is processed to complex-type structures supports the supposition that the degree of processing which individual oligosaccharides undergo is site specific (23, 24).

**Effect of temperature on transport of the HA glycosylation mutants.** Since it has been found that alterations in the glycosylation of HA that lead to misfolding and impaired transport can be partially alleviated by a reduction in temperature (14, 15, 39, 54), we tested the effect of reduced temperature on intracellular transport of transport-defective cg1,2 and cg1,2,3 mutants (Fig. 6). As at 37°C, the cleavage rates of these mutants were determined in pulse-chase experiments at both 33 and 40°C and compared with that of the vaccinia virus-expressed wild-type HA. To examine degradation of HA protein which might occur, we chose longer chase periods than those used at 37°C (Fig. 3 and 4). Immunoprecipitates were prepared from both cell extracts

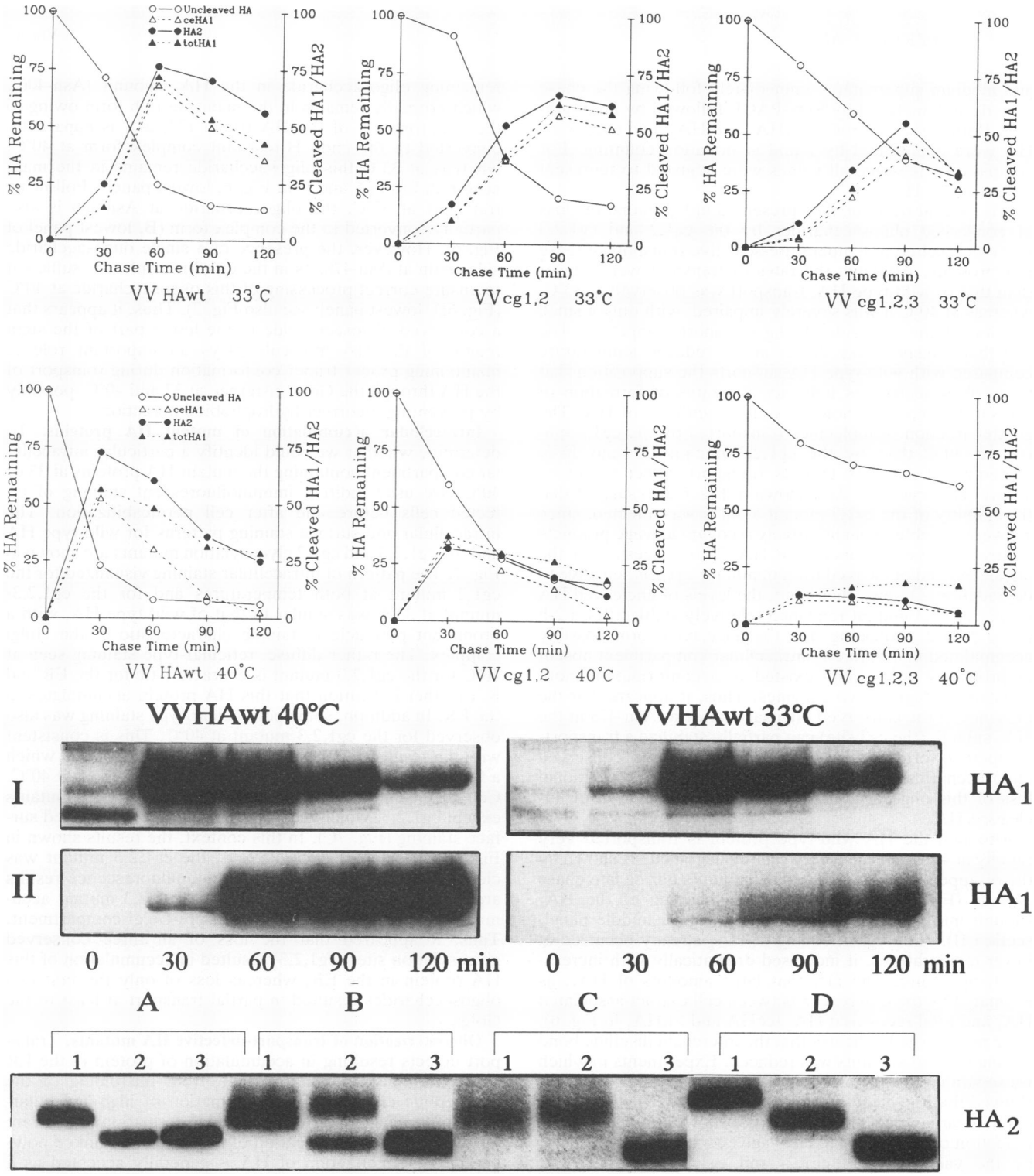


FIG. 6. Effect of temperature on intracellular transport of wild-type HA (HAwt) and HA glycosylation mutants. Dishes of CV-1 cells infected with the wild-type HA recombinant vaccinia virus (VV) and the cg1,2 and cg1,2,3 mutants were pulse-labeled with 100 μCi of L-[$^{35}$S]methionine for 10 min at either 33 or 40°C and then incubated in excess unlabeled methionine for the times indicated at the respective temperatures. HA proteins were immunoprecipitated from medium supernatants and cell extracts following lysis in a radioimmunoprecipitation assay with anti-FPV serum and subjected to SDS-PAGE. Upper panel: percentages of uncleaved HA versus cleaved HA determined at each time period by scintillation counting of HA bands isolated from dried gels. The following are shown in each graph with respect to time: HA, decline in uncleaved HA; $HA_2$, cleaved HA derived from the radioactivity found in $HA_2$ bands; $ceHA_1$, cleaved HA derived from $HA_1$ bands isolated from cell extracts; $totHA_1$, cleaved HA derived from both the $HA_1$ associated with cell extracts and the amount of $HA_1$ found in medium supernatants. The results are the mean values for each time period from at least two independent experiments. Middle panel: fluorograms of $HA_1$ immunoprecipitated from extracts (I) and medium supernatants (II) of cells infected with wild-type HA-producing vaccinia virus (see above). Lowest panel: three equal aliquots of immunoprecipitates of cg1,2 (D) and cg1,2,3 (A to C) mutant proteins after pulse-labeling (10 min) and a chase period of 60 min at 33°C (A), 37°C (B), or 40°C (C and D) left treated (lanes 1) or digested with endo H (lanes 2) or PNGase F (lanes 3) for 16 h at 37°C prior to SDS-PAGE and fluorography.

and medium supernatants immediately following the chase periods and analyzed by SDS-PAGE followed by fluorography. Both cleavage products ($HA_1$ and $HA_2$) and uncleaved HA were quantitated by liquid scintillation counting. For comparative reasons, all values were adjusted to represent total cleaved HA.

It is evident from the data presented in Fig. 6 that the loss of conserved oligosaccharides by the cg1,2 and cg1,2,3 mutants resulted in temperature-sensitive transport of these HA proteins. Although the rates of transport were slower than that of wild-type HA, transport was observed at 33°C, whereas at 40°C it was severely impaired, with only a small fraction of the molecules being transport competent. The fact that transport was slower at the reduced temperature compared with wild-type HA supports the supposition that these oligosaccharides influence the rates of formation of transport-competent molecules after synthesis of HA. The greater fraction of molecules transported by the cg1,2 mutant at 40°C than by the cg1,2,3 mutant (35 and 15%, respectively) suggests that its transport defect is not as severe. However, the data shown in Fig. 6 also suggest that the stability of the cg1,2 mutant at 40°C was affected, since we were not able to quantitatively recover cleavage products relative to levels of uncleaved HA. This suggests that the uncleaved and/or cleaved form of mutant cg1,2 is sensitive to degradation. On the other hand, the levels of uncleaved HA by the cg1,2,3 mutant remained relatively stable after a 2-h chase period, indicating that the uncleaved form possibly accumulated in a different intracellular compartment absent of proteases or possibly existed in a conformation more resistant to degradative enzymes. Thus, it appears that the presence of the conserved oligosaccharide at Asn-478 in the $HA_2$ subunit (the cg3 site) can partially stabilize a transport-competent form of HA after loss of the two conserved oligosaccharides in the $HA_1$ subunit, whereas the additional loss of this oligosaccharide results in accumulation of uncleaved HA.

Although the HA wild-type protein is transported very rapidly at 40°C, it is also very rapidly degraded, as shown by the disappearance of cleaved HA subunits during late chase periods (Fig. 6, upper panel) and shedding of the $HA_1$ subunit into the chase supernatants (Fig. 6, middle panel, section II). Although shedding of $HA_1$ already occurred at lower temperatures, it increased dramatically with increasing temperature. The fact that large amounts of $HA_1$, as estimated by the differences between cell extract-associated $HA_1$ and total recovered $HA_1$ (ceHA and tot$HA_1$ in Fig. 6), were readily shed indicates that the interchain disulfide bond linking the two subunits was reduced. Experiments in which we separated the HA proteins under nonreducing conditions showed that the cleavage products are linked via a disulfide bond at earlier chase times (data not shown), indicating that reduction occurs after the cleavage event. Shedding of $HA_1$ by the vaccinia virus cg1,2- and cg1,2,3-expressed HA proteins was also observed, suggesting that the level of shed $HA_1$ represents the fraction of molecules which are eventually transported to the plasma membrane. Immunoprecipitated $HA_1$ from medium supernatants and cell extract-associated $HA_1$ displayed similar electrophoretic mobilities, which implies that unspecific proteolysis is not responsible for the dissociation of HA subunits.

The transport-competent form of the cg1,2,3 mutant also displayed temperature-sensitive processing of the remaining oligosaccharides. At the restrictive temperature, the $HA_2$ subunit of the cg1,2,3 mutant migrated more slowly than the equivalent form found at that permissive temperature. The remaining oligosaccharide in the $HA_2$ subunit (Asn-406), which normally remains in the mannose-rich form owing to the conformation of the HA trimer (23, 24), is apparently converted to the endo H-resistant complex form at 40°C, whereas at 33°C this oligosaccharide remains in the mannose-rich form (A and C in Fig. 6, lowest panel). Following transport at 37°C, the oligosaccharide at Asn-406 is also partially converted to the complex form (B, lowest panel of Fig. 6). However, the presence of a single oligosaccharide side chain at Asn-478, as in the cg1,2 mutant, was sufficient to ensure correct processing of this oligosaccharide at 40°C (Fig. 6D, lowest panel; see also Fig. 7). Thus, it appears that a conserved oligosaccharide in the lower part of the stem region of the HA molecule plays an important role in maintaining proper trimer conformation during transport of the HA through the Golgi cisternae at 37 and 40°C, possibly by preventing incorrect hydrophobic interactions.

**Intracellular accumulation of mutant HA proteins.** To determine whether we could identify a particular intracellular compartment containing the mutant HA proteins at 33 or 40°C, we used indirect immunofluorescent staining of infected cells before and after cell permeabilization. The intracellular and surface staining patterns for wild-type HA and the cg1,2,3 and cg1,2 glycosylation mutants are shown in Fig. 7. The pattern of intracellular staining visualized for the cg1,2 mutant at both temperatures and for the cg1,2,3-mutant at 33°C was similar to that of wild-type HA, with a prominent perinuclear staining characteristic of the Golgi complex. The rather diffuse, reticular-type staining seen at 40°C for the cg1,2,3 mutant is characteristic for the ER and is a further indication that this HA protein accumulates in the ER. In addition, some perinuclear-type staining was also observed for the cg1,2,3 mutant at 40°C. This is consistent with the results of the kinetic experiments (Fig. 6), in which a fraction of the cg1,2,3 protein was found cleaved at 40°C. Cell surface expression was found with all of the mutants except cg1,2,3, which displayed significantly decreased surface staining (Fig. 7C). In this context, the results shown in Fig. 6 suggested that ca. 15% of the cg1,2,3 mutant was cleaved at 40°C. Although the immunofluorescence results are qualitative, they suggest that the cg1,2,3 mutant accumulated mainly intracellularly in a pre-Golgi compartment. Thus, it appeared that the loss of all three conserved glycosylation sites (cg1,2,3) resulted in accumulation of this HA protein in the ER, whereas loss of only the first two oligosaccharides resulted in partial transport at least to the Golgi.

**Oligomerization of transport-defective HA mutants.** Transport defects resulting in accumulation of protein in the ER have often been found to result from misfolding of the polypeptide chain leading to formation of high-molecular-weight aggregates. This may be due to formation of aberrant disulfide bonds or aggregation of noncovalently linked polypeptides. Trimerization of HA is generally accepted as a prerequisite for transport from the ER to the Golgi compartments (9, 15, 16, 19, 54). Therefore, it is likely that trimerization or an earlier event, such as folding, is impaired with the cg1,2,3 mutant. On the other hand, we would expect that the cg1,2 mutant exists mainly in a trimerized form that, although unstable, is at least partially transport competent. To examine the temperature-sensitive effects on the oligomerization of these mutant HA proteins, we analyzed labeled HA proteins after a pulse-chase experiment similar to that whose results are presented in Fig. 6 by sucrose gradient centrifugation. Fractions were collected from the bottom of the gradients, subjected to immunoprecipitation,

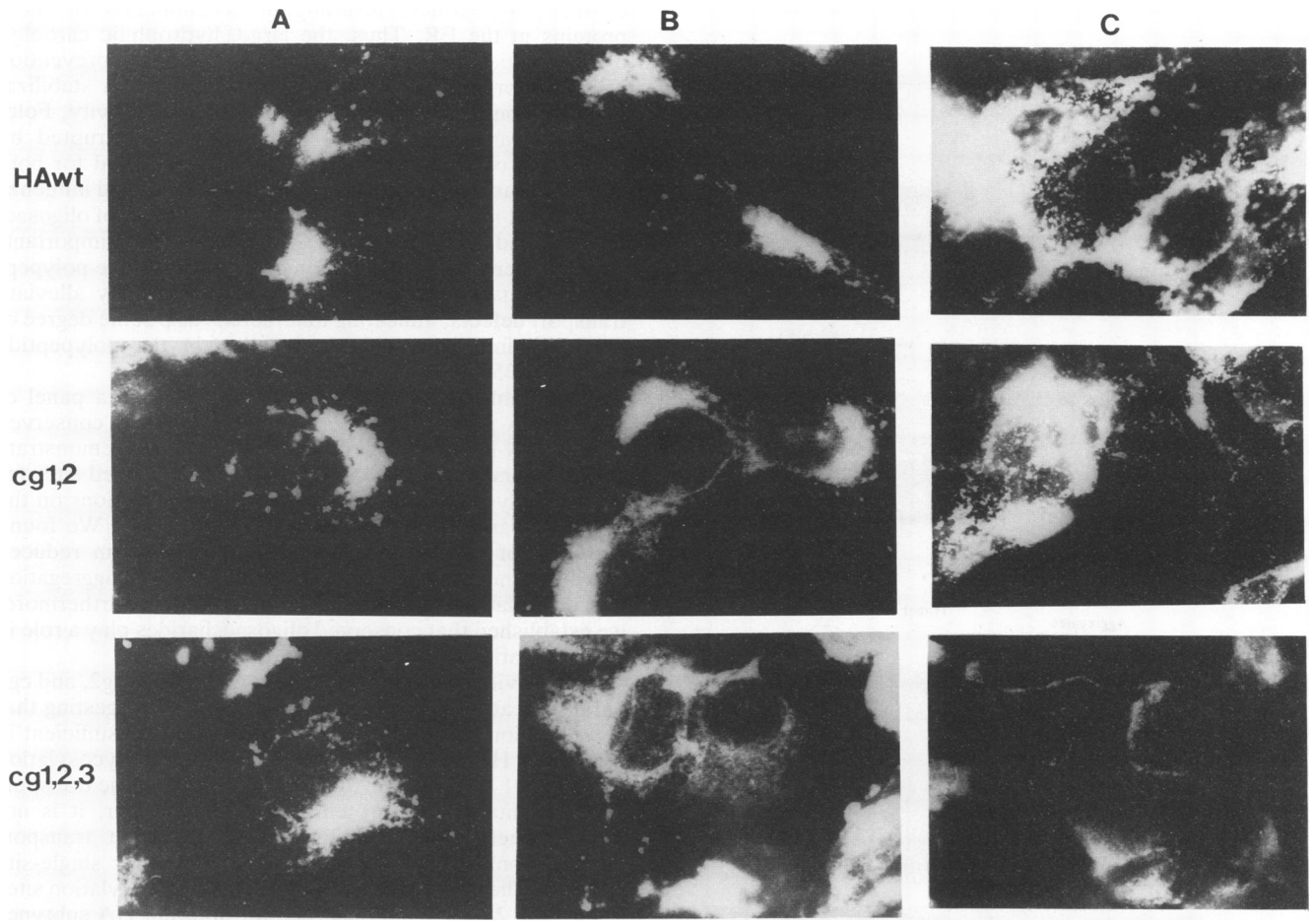


FIG. 7. Indirect immunofluorescence of temperature-sensitive mutants and the wild type. Coverslips containing vaccinia virus recombinant-infected CV-1 cells at 6 h postinfection were fixed and/or permeabilized; this was followed by indirect immunofluorescent staining of HA-specific proteins. Results of intracellular staining of vaccinia virus wild-type HA and cg1,2 and cg1,2,3 mutant-expressed HA proteins at 33°C (A) and 40°C (B) and surface staining at 40°C (C) are shown.

and analyzed by SDS-PAGE under reducing conditions. The results of this experiment are presented in Fig. 8. As can be seen for the wild-type HA after 10 min of pulse-labeling at 40°C, HA was concentrated in fractions isolated from the top of the gradient. Most of the protein found immediately after the pulse was concentrated in three fractions which are indicative of monomeric HA, whereas the faster migrating bands represent trimeric HA which occurs soon after protein synthesis (4, 8, 9, 15, 16). After a chase period of 60 min, most of the HA protein migrated in the trimeric fractions and was effectively transported to Golgi compartments, as indicated by cleavage of the HA. The data for wild-type HA at 33°C were similar and were therefore omitted. The HA protein of the cg1,2,3 mutant displayed different oligomeric forms at the two temperatures. Whereas the cg1,2,3 protein was able to trimerize at 33°C, it migrated throughout the entire gradient at 40°C, indicating the formation of aggregates of various higher molecular weights. Only small amounts of these aggregates were present at the lower temperature. Thus, it appears that the large reduction of transported HA protein by this mutant is the result of misfolded protein leading to formation of aggregates. On the other hand, aggregation was not observed at 40°C with the cg1,2 mutant. The rapid decline in the levels of uncleaved HA after a 60-min chase period are not commensurate with an increase in the levels of cleaved HA, as was also seen in the kinetic experiments (Fig. 6), and suggests that uncleaved cg1,2 HA is subjected to rapid degradation. These results suggest that the oligosaccharides at conserved sites promote proper trimerization, probably by promoting a trimerization-competent form of the monomer. Taken together, the temperature-sensitive phenotype of these mutants supports the view that the role of conserved N-linked glycans on the HA is to aid in proper folding of the molecule.

## DISCUSSION

Oligonucleotide-directed mutagenesis has been used to study the roles of individual oligosaccharides in a wide variety of secretory and membrane-bound glycoproteins, including vesicular stomatitis virus G protein (35, 49), hemagglutinin-neuraminidase of simian virus 5 (42), human immunodeficiency virus gp41 (11), human protein C (18), and human chorionic gonadotropin (38). Although the results of these studies varied with respect to the proteins studied, loss of specific oligosaccharides was found to affect either transport or the biological activities of these proteins. Transport defects were suggested to be largely due to aberrant folding

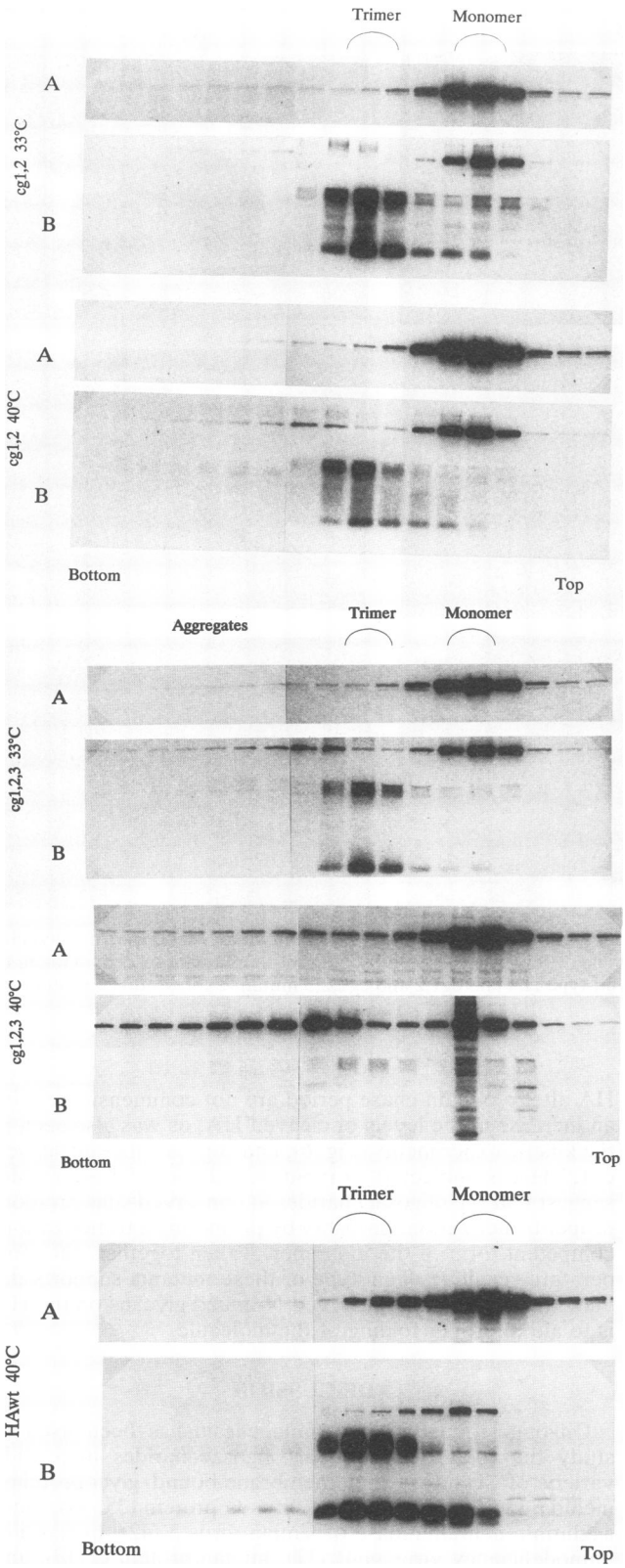


FIG. 8. Velocity gradient centrifugation of temperature-sensitive mutant HA. At 3.5 h postinfection, recombinant virus-infected CV-1 cells were labeled with [$^{35}$S]methionine for 10 min and harvested immediately (A) or chased for 60 min at 33 or at 40°C (B) in the presence of excess unlabeled methionine. Detergent cell extracts were loaded on 5 to 25% sucrose gradients and subjected to centrifugation at 36,000 rpm (SW41; Beckman) for 16 h at 20°C. Fractions were collected from the bottom of each gradient and immunoprecipitated with anti-FPV serum. Immunoprecipitates were analyzed by SDS-PAGE under reducing conditions. The HA monomer and trimer correspond to fractions 17 to 19 and 13 to 15, respectively. Fractions 1 to 4 and 23 and 24 have been omitted. Panels: top, HA of pulse (A) and HA, $HA_1$, and $HA_2$ of pulse-chase experiments (B) with vaccinia virus cg1,2,3 mutant at 33 and 40°C; middle, vaccinia virus cg1,2 mutant at 33 and 40°C; bottom, vaccinia virus wild-type HA (HAwt) at 40°C.

of the polypeptides, resulting in accumulation of these proteins in the ER. Thus, the large, hydrophilic carbohydrate moieties may aid in either protein folding, prevention of inappropriate hydrophobic interactions, and/or stabilization of a conformation suitable for biological activity. Folding and transport of proteins can also be disrupted by alterations of the glycosylation sites, as observed for both the vesicular stomatitis virus G protein (12, 34) and influenza virus HA (14, 15, 54), suggesting that the number of oligosaccharides and their locations in the polypeptide are important. On the other hand, introduction of new sites in the polypeptide chain lacking the original sites can partially alleviate transport defects, indicating that there is also some degree of flexibility in oligosaccharide location in the polypeptide chain (34, 35, 49).

In this study, we constructed and expressed a panel of mutant HA proteins lacking one or more of the conserved sites for N-linked glycosylation. Our results demonstrate that the number of carbohydrates at the conserved sites for N-linked glycosylation and their respective locations on the molecule can influence HA transport (Table 1). We found that loss of specific oligosaccharides resulted in reduced assembly and cleavage rates and induced protein aggregation and degradation of the mutant HA proteins. Furthermore, we established that conserved oligosaccharides play a role in the modulation of final carbohydrate structures.

The individual loss of glycosylation sites cg1, cg2, and cg3 did not greatly affect efficiency of transport, suggesting that glycosylation at two of the conserved sites was sufficient in promoting HA transport. Elimination of each glycosylation site on X-31 HA (52) also did not seem to affect the transport of those mutant HA proteins greatly. However, it is not known whether these mutant proteins exhibit transport kinetics comparable to those reported here for single-site mutants. The individual loss of conserved glycosylation sites at position 28 has been observed for different HA subtypes and their variants, apparently without having any deleterious effect on virus propagation and the transport of these proteins. Loss of the carbohydrate at position 12 (Asn-11 and Asn-22 with serotypes H5 and H3, respectively) has been shown to play an important role in the maturation of H5 and H3 HA proteins by enhancing cleavage of variants or mutants of these proteins (20, 44, 64). On the other hand, this apparent masking effect of the cleavage site by the cg1 oligosaccharide can be alleviated by modification of the cleavage site (44, 64). The presence or absence of this oligosaccharide on H7 FPV HA had no detectable effect on the cleavability of the HA proteins.

There has been no report of an HA protein which lacks more than one conserved site for N-glycosylation. This might suggest that there is selective pressure during evolution against the loss of more than one conserved site. However, when conserved glycosylation was restricted to

TABLE 1. Transport characteristics of the wild type and glycosylation mutants

| Glycosylation site(s) mutated | $t_{1/2}$[a] of cleavage (min) | | | % Transport competent[b] | | | Cell surface expression[c] | | |
|---|---|---|---|---|---|---|---|---|---|
| | 33°C | 37°C | 40°C | 33°C | 37°C | 40°C | 33°C | 37°C | 40°C |
| None (wild type) | 44 | 30 | 20 | 76 | 85 | 90 | ++ | ++ | ++ |
| cg1 | ND[d] | 34 | ND | ND | 88 | ND | ND | ++ | ND |
| cg2 | ND | 45 | ND | ND | 67 | ND | ND | ++ | ND |
| cg3 | ND | 33 | ND | ND | 88 | ND | ND | ++ | ND |
| $cg3^{+4}$ | ND | 41 | ND | ND | 75 | ND | ND | ++ | ND |
| cg1,3 | ND | 55 | ND | ND | 77 | ND | ND | ++ | ND |
| cg2,3 | ND | 55 | ND | ND | 62 | ND | ND | ++ | ND |
| cg1,2 | 55 | 48[e] | 39[e] | 62 | 30 | 30 | ++ | + | + |
| cg1,2,3 | 78 | Aggr.[f] | Aggr. | 35 | 20 | 12 | ++ | + | ± |

[a] $t_{1/2}$, half-time.
[b] Values are from Fig. 3 and 6.
[c] Detected by immunostaining. Staining: ++, strong; +, weak; ±, very weak.
[d] ND, not determined.
[e] HA is partially proteolytically degraded ($HA_1$ and $HA_2$, ≤33%.
[f] Aggr., aggregation.

either position 12 or 28, the efficiency of transport was not greatly affected. Thus, it seems reasonable to assume that natural HA variants possessing conserved glycosylation at only one of these positions exist. Alternatively, these mutants might possess deleterious structural features that are selected against for reasons which we were unable to ascertain with the approach described here. That the oligosaccharides at conserved sites represent important structural elements is indicated by the finding that they are also present in HA of influenza B virus.

Our data suggest that the conserved sites at residues 12 and 28 are crucial for maintenance of proper assembly and efficient transport of mutant HA proteins. Conserved glycosylation restricted to either of these sites can promote efficient HA transport, albeit at significantly reduced rates compared with wild-type HA or single-site mutants. This implies that two oligosaccharides at conserved sites function synergistically in promoting and enhancing HA assembly and transport. On the other hand, the cg3 oligosaccharide is not able to compensate completely for loss of oligosaccharides at other conserved sites. The transport of the cg1,2 mutant and the mutant lacking all three sites is temperature sensitive. Only a small fraction of the cg1,2 and cg1,2,3 mutant molecules (ca. 15 and 35%, respectively) is capable of proper assembly and is found cleaved at 37 or 40°C, whereas this fraction increases two- to fourfold at 33°C. Two different fates were observed for the transport-incompetent forms of these mutants at 40°C. Most of the cg1,2,3 polypeptides accumulated in heterogeneous complexes of various molecular weights. After chase periods of 60 and 120 min, most of the cg1,2,3 mutant was core glycosylated and uncleaved, suggesting that, indeed, these aggregates are not transport competent. Immunofluorescent staining of permeabilized cells infected with the vaccinia virus cg1,2,3 mutant also revealed extensive reticular-type staining, indicative of ER accumulation at 40°C. Aggregation of the cg1,2 mutant was not observed, suggesting that the cg3 oligosaccharide plays an important role in preventing protein aggregation. However, the cg1,2 mutant displayed rapid degradation compared with the relatively stabile aggregates of the cg1,2,3 mutant. Levels of uncleaved cg1,2 disappeared with time without being converted to the cleaved form. It is possible that misfolding of the cg1,2 molecules exposes surface determinants that direct these molecules to a compartment specialized for rapid degradation (1, 6, 32). In this respect, the aggregation of HA molecules might protect these forms from rapid degradation by masking such determinants or by masking protease-sensitive peptide regions.

An interesting aspect of HA transport derived from the present study is the finding that the $HA_1$ subunit of the wild-type HA protein was readily shed into the medium of recombinant vaccinia virus-infected cells, suggesting that the disulfide-linked subunits had been reduced. Reduction of cleaved HA was not found at earlier chase times (data not shown), and this indicates that reduction occurs after cleavage, probably in vesicles destined for the plasma membrane. Furthermore, we detected no difference in the mobilities of $HA_1$ derived from cell extracts and medium-associated $HA_1$, implying that unspecific proteolysis of $HA_1$ is not responsible for dissociation of subunits. Recently it has been reported that the cleaved form of FPV HA in influenza virus-infected cells undergoes an acid-induced conformational change late in transport, when the function of the viral $M_2$ protein is inhibited by amantadine (61). The $M_2$ protein appears to function as an ion channel which regulates the pH of the trans-Golgi network and/or transport vesicles destined for the plasma membrane (7, 61). These studies revealed that inhibition of $M_2$ with amantadine leads to an acid-induced conformational change in the HA protein. The low-pH form of cleaved HA was very sensitive to reducing agents, e.g., dithiothreitol, which in turn resulted in shedding of the $HA_1$ subunit into the medium. On the basis of these findings, one would expect that expression of FPV HA without $M_2$ would result in conversion of the cleaved HA to a low-pH form. Although we do not have direct evidence that vaccinia virus-expressed FPV HA undergoes a pH-induced conformational change, shedding of the $HA_1$ subunit and degradation of the $HA_2$ subunit might be explained by such an alteration. However, the mechanism behind the reduction of the disulfide-linked subunits remains obscure, since reducing agents were not included in the labeling medium. In vivo susceptibility of this disulfide bond for reduction is observed only after cleavage and exposure of the HA to a low pH (17). In addition, Skibbens and coworkers (58) have reported that reduction of such a bond can occur in vitro late in transport and only after the HA has been cleaved. We are currently investigating the precise site where reduction occurs and whether coexpression of HA with the $M_2$ protein can alleviate these effects.

We also took advantage of the known carbohydrate struc-

tures found at each individual site for glycosylation of FPV HA (23) to address some of the factors that influence final carbohydrate structures on proteins. Our panel of mutant proteins were a valuable source in determining some of these factors. Loss of the cg1 site for glycosylation apparently allows complete processing of the neighboring oligosaccharide at position 28, whereas its presence results in only partial processing of the Asn-28-linked oligosaccharide. These results confirm our previous data (23), which show that both oligomannosidic- and complex-type structures are found at the cg2 site for glycosylation. This effect appears to result from steric hindrance due to the cg1 site and not from carbohydrate interactions with the cg3 site, which is also in close proximity to both of these oligosaccharides (Fig. 1A). In contrast to the complex endo H-resistant structure found at residue 478 (cg3 site), the novel site introduced only 4 amino acids away, at residue 482, possessed an endo H-sensitive structure, suggesting that the processing of this oligosaccharide is arrested in the mannose-rich form. Interestingly, we also noted that there were variations in the processing of remaining carbohydrates on HA lacking all three conserved sites. The $HA_2$ subunit derived from the small fraction of transport-competent cg1,2,3-HA at 37 and 40°C displayed altered mobilities compared with that observed at 33°C. Previous reports have shown that the mannose-rich form of the Asn-406-linked oligosaccharide in the $HA_2$ subunit is due to its being buried in niches of trimer interface surfaces found at the upper stem domain of the molecule (24); this implies that the inaccessibility of this site for trimming and processing of enzymes is a direct consequence of trimer conformation. Thus, it seems that conversion of this normally mannose-rich oligosaccharide to a complex endo H-resistant structure is the direct result of conformational relaxation due to loss of conserved oligosaccharides in the lower stem region of the molecule. Both reduced temperature and the presence of a single conserved oligosaccharide are sufficient for maintenance of the proper conformation, which blocks accessibility of this oligosaccharide for processing enzymes.

In summary, the primary role of conserved HA glycans appears to be in promoting proper folding and assembly of the HA molecules and protecting the HA protein from aggregation and proteolytic degradation. The conserved glycans act synergistically to enhance both the rate and efficiency of folding and assembly of HA, a prerequisite for intracellular transport of HA out of the ER. The amino-terminal oligosaccharides at positions 12 (cg1) and 28 (cg3) are crucial for maintenance of assembly and transport. Both sites are important for prevention of proteolytic degradation early after synthesis, whereas the oligosaccharide at position 478 (cg3 site) preferentially plays a role in preventing aggregation of polypeptides.

## ACKNOWLEDGMENTS

We are grateful to Evelyne Kretzschmar and Kazumichi Kuroda for providing the HA gene of FPV cloned in the M13 phage; B. Moss, Laboratory of Viral Diseases, NIAID, Bethesda, Md., for vaccinia virus vector pSC11; and J. Hegemann, Institut für Mikrobiologie, Justus-Liebig-Universität Giessen, Germany, for synthesizing the oligonucleotides.

This work was supported by the Deutsche Forschungsgemeinschaft (SFB 286) and the Fonds der Chemischen Industrie.

## ADDENDUM

After submission of the manuscript, a study on glycosylation of H3 HA leading to similar conclusions was published (14a).

## REFERENCES

1. **Amara, J. E., G. Lederkremer, and H. F. Lodish.** 1989. Intracellular degradation of unassembled asialoglycoprotein receptor units: a pre-Golgi, nonlysosomal endoproteolytic cleavage. J. Cell Biol. **109:**3315–3324.
2. **Bennett, M. K., A. Wandinger-Ness, and K. Simons.** 1988. Release of exocytic transport vesicles from perforated MDCK cells. EMBO J. **7:**4075–4085.
3. **Boulay, F., R. W. Doms, R. Webster, and A. Helenius.** 1988. Posttranslational oligomerization and cooperative acid-activation of mixed influenza hemagglutinin trimers. J. Cell Biol. **106:**629–639.
4. **Braakman, I., H. Hoover-Litty, K. R. Wagner, and A. Helenius.** 1991. Folding of influenza hemagglutinin in the endoplasmic reticulum. J. Cell Biol. **114:**401–411.
5. **Chakrabarti, S., K. Brechling, and B. Moss.** 1985. Vaccinia virus expression vector: coexpression of β-galactosidase provides visual screening of recombinant virus plaques. Mol. Cell. Biol. **5:**3403–3409.
6. **Chen, C., J. S. Bonifacino, L. Yuan, and R. D. Klausner.** 1988. Selective degradation of T cell antigen receptor chains retained in a pre-Golgi compartment. J. Cell Biol. **107:**2149–2161.
7. **Ciampor, F., P. M. Baley, M. V. Nermut, E. M. A. Hirst, R. J. Sugrue, and A. J. Hay.** 1992. Evidence that the amantadine-induced, M2-mediated conversion of influenza A virus hemagglutinin to the low conformation occurs in an acidic trans Golgi compartment. Virology **186:**14–24.
8. **Copeland, C. S., R. W. Doms, E. M. Bolzau, R. G. Webster, and A. Helenius.** 1986. Assembly of influenza hemagglutinin trimers and its role in intracellular transport. J. Cell Biol. **103:**1179–1191.
9. **Copeland, C. S., K.-O. Zimmer, K. R. Wagner, G. A. Healey, I. Mellman, and A. Helenius.** 1988. Folding, trimerization and transport are sequential events in the biogenesis of influenza virus hemagglutinin. Cell **53:**197–209.
10. **De Curtis, I., and K. Simons.** 1989. Isolation of exocytic carrier vesicles from BHK cells. Cell **58:**719–727.
11. **Dedera, D. A., R. Gu, and L. Ratner.** 1992. Role of asparagine-linked glycosylation in human immunodeficiency virus type 1 transmembrane envelope function. Virology **187:**377–382.
12. **Doms, R. W., A. Ruusala, C. Machamer, J. Helenius, A. Helenius, and J. K. Rose.** 1988. Different effects of mutations in three domains on folding, quaternary structure, and intracellular transport of vesicular stomatitis virus G protein. J. Cell Biol. **107:**89–99.
13. **Elbein, A. D.** 1987. Inhibitors of the biosynthesis and processing of N-linked oligosaccharide chains. Annu. Rev. Biochem. **56:**497–534.
14. **Gallagher, P., J. Henneberry, I. Wilson, J. Sambrook, and M.-J. Gething.** 1988. Addition of carbohydrate side chains at novel sites on influenza virus hemagglutinin can modulate the folding, transport, and activity of the molecule. J. Cell Biol. **107:**2059–2073.

14a. **Gallagher, P. J., J. M. Henneberry, J. F. Sambrook, and M.-J. H. Gething.** 1992. Glycosylation requirements for intracellular transport and function of the hemagglutinin of influenza virus. J. Virol. **66:**7136–7145.

15. **Garten, W., C. Will, K. Buckard, K. Kuroda, D. Ortmann, K. Munk, C. Scholtissek, H. Schnittler, D. Drenckhahn, and H.-D. Klenk.** 1992. Structure and assembly of hemagglutinin mutants of fowl plague virus with impaired surface transport. J. Virol. **66:**1495–1505.
16. **Gething, M.-J., K. McCammon, and J. Sambrook.** 1986. Expression of wild-type and mutant forms of influenza hemagglutinin: the role of folding in intracellular transport. Cell **46:**939–950.
17. **Graves, P. N., J. L. Schulman, J. F. Young, and P. Palese.** 1983. Preparation of influenza virus subviral particles lacking the HA1

subunit of hemagglutinin: unmasking of cross-reactive HA2 determinants. Virology **126:**106–116.
18. **Grinnell, B. W., J. D. Walls, and B. Gerlitz.** 1991. Glycosylation of human protein C affects its secretion, processing, functional activities, and activation by thrombin. J. Biol. Chem. **226:**9778–9785.
19. **Hurtley, S. M., D. G. Bole, H. Hoover-Litty, A. Helenius, and C. S. Copeland.** 1989. Interactions of misfolded influenza virus hemagglutinin with binding protein (BiP). J. Cell Biol. **108:**2117–2126.
20. **Kawaoka, Y., C. W. Naeve, and R. G. Webster.** 1984. Is virulence of H5N2 influenza viruses in chickens associated with loss of carbohydrate from the hemagglutinin? Virology **139:**303–316.
21. **Kawaoka, Y., and R. G. Webster.** 1989. Interplay between carbohydrate in the stalk and the length of the connecting peptide determines the cleavability of influenza virus hemagglutinin. J. Virol. **63:**3296–3300.
22. **Kawaoka, Y., S. Yamnikova, T. M. Chambers, D. K. Lvov, and R. G. Webster.** 1990. Molecular characterization of a new hemagglutinin, subtype H 14, of influenza A virus. Virology **179:**759–767.
23. **Keil, W., R. Geyer, I. Dabrowski, U. Dabrowski, H. Niemann, S. Stirm, and H.-D. Klenk.** 1985. Carbohydrates of influenza virus. VI. Structural elucidation of the individual glycans of the FPV hemagglutinin by two dimensional $^1$H n.m.r. and methylation analysis. EMBO J. **4:**2711–2720.
24. **Keil, W., H. Niemann, R. T. Schwarz, and H.-D. Klenk.** 1984. Carbohydrates of influenza virus. V. Oligosaccharides attached to individual glycosylation sites of hemagglutinin of fowl plague virus. Virology **133:**77–91.
25. **Klenk, H.-D.** 1990. Influence of glycosylation on antigenicity of viral proteins, p. 25–37. *In* (M. H. V. van Regenmortel and A. R. Neurath (ed.), Immunochemistry of viruses II. Elsevier, Amsterdam.
26. **Klenk, H.-D., and R. Rott.** 1973. Formation of influenza virus proteins. J. Virol. **11:**823–831.
27. **Klenk, H.-D., and R. Rott.** 1988. The molecular basis of influenza virus pathogenicity. Adv. Virus Res. **34:**247–281.
28. **Kornfeld, R., and S. Kornfeld.** 1985. Assembly of asparagine-linked oligosaccharides. Annu. Rev. Biochem. **54:**631–664.
29. **Kuroda, K., C. Hauser, R. Rott, H.-D. Klenk, and W. Doerfler.** 1986. Expression of the influenza virus haemagglutinin in insect cells by a baculovirus vector. EMBO J. **5:**1359–1365.
30. **Kuroda, K., M. Veit, and H.-D. Klenk.** 1991. Retarded processing of influenza virus hemagglutinin in insect cells. Virology **180:**159–165.
31. **Laemmli, U. K.** 1970. Cleavage of structural proteins during the assembly of the head of bacteriophage T4. Nature (London) **227:**680–685.
32. **Lippincott-Schwartz, J., J. S. Bonifacino, L. Yuan, and R. Klausner.** 1988. Degradation from the endoplasmic reticulum: disposing of newly synthesized proteins. Cell **54:**209–229.
33. **Lohmeyer, J., and H.-D. Klenk.** 1979. Temperature-sensitive defect in the posttranslational processing of the hemagglutinin. Virology **93:**134–145.
34. **Machamer, C. E., and J. K. Rose.** 1988. Influence of new glycosylation sites on expression of the vesicular stomatitis virus G protein at the plasma membrane. J. Biol. Chem. **263:**5948–5954.
35. **Machamer, C. E., and J. K. Rose.** 1988. Vesicular stomatitis virus G proteins with altered glycosylation sites display temperature-sensitive intracellular transport and are subject to aberrant intermolecular disulfide bonding. J. Biol. Chem. **263:**5955–5960.
36. **Mackett, M., G. L. Smith, and B. Moss.** 1984. General method for production and selection of infectious vaccinia virus recombinants expressing foreign genes. J. Virol. **49:**857–864.
37. **Matlin, K. S., and K. Simons.** 1983. Reduced temperature prevents transfer of a membrane glycoprotein to the cell surface but does not prevent terminal glycosylation. Cell **34:**233–243.
38. **Matzuk, M., and I. Boime.** 1988. The role of asparagine-linked oligosaccharides of the alpha-subunit in the secretion and assembly of human chorionic gonadotropin. J. Cell Biol. **106:**1049–1059.
39. **Mücke, K., and C. Scholtissek.** 1987. Extragenic and intragenic suppression of a transport mutation in the hemagglutinin gene of an influenza A virus as revealed by backcross and sequence determination. Virology **158:**112–117.
40. **Munk, K., E. Pritzer, E. Kretzschmar, B. Gutte, W. Garten, and H.-D. Klenk.** 1992. Carbohydrate masking of an antigenic epitope of influenza virus hemagglutinin independent of oligosaccharide size. Glycobiology **2:**233–240.
41. **Naeve, C. W., and D. Williams.** 1990. Fatty acids on the A/Japan/305/57 influenza virus hemagglutinin have a role in membrane fusion. EMBO J. **9:**3857–3866.
42. **Ng, D. T. W., S. W. Hiebert, and R. A. Lamb.** 1990. Different roles of individual N-linked oligosaccharide chains in folding, assembly, and transport of simian virus 5 hemagglutinin-neuraminidase. Mol. Cell. Biol. **10:**1989–2001.
43. **Nobusawa, E., T. Aoyama, H. Kato, Y. Suzuki, Y. Tateno, and K. Nakajima.** 1991. Comparison of complete amino acid sequences and receptor-binding properties among 13 serotypes of hemagglutinins of influenza viruses. Virology **182:**475–485.
44. **Ohuchi, M., M. Orlich, R. Ohuchi, B. E. J. Simpson, W. Garten, H.-D. Klenk, and R. Rott.** 1989. Mutations at the cleavage site of hemagglutinin alter the pathogenicity of influenza virus A/chick/Penn/83 (H5N2). Virology **168:**274–280.
45. **Ohuchi, R., M. Ohuchi, W. Garten, and H.-D. Klenk.** 1991. Hemagglutinin of human influenza virus with high sensitivity to proteolytic activation. J. Virol. **65:**3530–3557.
46. **Olden, K., B. A. Bernand, M. J. Humphries, T.-K. Yeo, S. L. White, S. A. Newton, H. C. Bauer, and J. B. Parent.** 1985. Functions of glycoprotein glycans. Trends Biochem. Sci. **3:**78–82.
47. **Olden, K., J. B. Parent, and S. L. White.** 1982. Carbohydrate moieties of glycoproteins. A re-evaluation of their function. Biochim. Biophys. Acta **650:**209–232.
48. **Orlich, M., D. Khatchikian, A. Teigler, and R. Rott.** 1990. Structural variation occurring in the influenza virus A/turkey/Oregon/71 during adaptation to different cell types. Virology **176:**531–538.
49. **Pitta, A. M., J. K. Rose, and C. E. Machamer.** 1989. A single-amino-acid substitution eliminates the stringent carbohydrate requirement for intracellular transport of viral glycoprotein. J. Virol. **63:**3801–3809.
50. **Porter, A. G., C. Barber, N. H. Carey, R. A. Hallewell, G. Threlfall, and J. S. Emtage.** 1979. Complete nucleotide sequence of an influenza hemagglutinin gene from cloned DNA. Nature (London) **282:**471–477.
51. **Robertson, J. S., R. Bootman, R. Newman, J. S. Oxford, R. S. Daniels, R. G. Webster, and G. C. Schild.** 1987. Structural changes in the haemagglutinin which accompany egg adaptation of an influenza A (H1N1) virus. Virology **160:**31–37.
52. **Roth, G. M., M.-J. Gething, and J. Sambrook.** 1989. Membrane insertion and intracellular transport of influenza virus glycoproteins, p. 219–267. *In* R. M. Krug (ed.), The influenza viruses. Plenum Press, New York.
53. **Sanger, F., S. Nicklen, and A. R. Coulson.** 1977. DNA sequencing with chain-terminating inhibitors. Proc. Natl. Acad. Sci. USA **74:**5463–5467.
54. **Schuy, W., C. Will, K. Kuroda, C. Scholtissek, W. Garten, and H.-D. Klenk.** 1986. Mutations blocking the transport of the influenza virus hemagglutinin between the rough endoplasmic reticulum and the Golgi apparatus. EMBO J. **5:**2831–2836.
55. **Schwarz, R. T., and R. Datema.** 1984. Inhibitors of trimming: new tools in glycoprotein research. Trends Biochem. Sci. **9:**32–34.
56. **Sharon, N.** 1984. Glycoproteins. Trends Biochem. Sci. **1:**198–202.
57. **Skehel, J. J., D. J. Stevens, R. S. Daniels, A. R. Douglas, M. Knossow, I. A. Wilson, and D. C. Wiley.** 1984. A carbohydrate side chain on hemagglutinins of Hong Kong influenza viruses inhibits recognition by a monoclonal antibody. Proc. Natl. Acad. Sci. USA **81:**1779–1783.
58. **Skibbens, J. E., M. Roth, and K. S. Matlin.** 1989. Differential

extractability of influenza virus hemagglutinin during intracellular transport in polarized epithelial cells and nonpolar fibroblasts. J. Cell Biol. **108:**821–832.

59. **Steinhauer, D. S., S. A. Wharton, D. C. Wiley, and J. J. Skehel.** 1991. Deacylation of hemagglutinin of A/Aichi/2/68 has no effect on membrane fusion properties. Virology **184:**445–448.
60. **Stieneke-Gröber, A., M. Vey, H. Angliker, E. Shaw, G. Thomas, C. Roberts, H.-D. Klenk, and W. Garten.** 1992. Influenza virus hemagglutinin with multibasic cleavage site is activated by furin, a subtilisin-like endoprotease. EMBO J. **11:**2407–2414.
61. **Sugrue, R. J., G. Bahadur, M. C. Zambon, M. Hall-Smith, A. R. Douglas, and A. J. Hay.** 1990. Specific structural alteration of influenza haemagglutinin by amantadine. EMBO J. **9:**3469–3476.
62. **Taylor, J. W., J. Ott, and F. Eckstein.** 1985. The rapid generation of oligonucleotide-directed mutations at high frequency using phosphorothioate-modified DNA. Nucleic Acids Res. **13:**8764–8785.
63. **Veit, M., E. Kretzschmar, K. Kuroda, W. Garten, M. F. G. Schmidt, H.-D. Klenk, and R. Rott.** 1991. Site-specific mutagenesis identifies three cysteine residues in the cytoplasmatic tail as acylation sites of influenza virus hemagglutinin. J. Virol. **65:**2491–2500.
64. **Webster, R. G., Y. Kawaoka, and W. J. Bean.** 1986. Molecular changes in A/chicken/Pennsylvania/83 (H5N2) influenza virus associated with acquisition of virulence. Virology **149:**165–173.
65. **Wiley, D. C., and J. J. Skehel.** 1987. The structure and function of the hemagglutinin membrane glycoprotein of influenza virus. Annu. Rev. Biochem. **56:**365–394.
66. **Wilson, I. A., J. J. Skehel, and D. C. Wiley.** 1981. Structure of the haemagglutinin membrane glycoprotein of influenza virus at 3 A resolution. Nature (London) **289:**366–373.